CHAPTER 38

Least Squares/Domain Imbedding Methods for Neumann Problems: Applications to Fluid Dynamics

E. J. Dean[1]
Q. V. Dinh[2]
R. Glowinski[3]
Jiwen He[4]
T. W. Pan[1]
J. Périaux[2]

Abstract

In this paper we discuss a domain imbedding (fictitious domain) methods which is well suited to the numerical solution of Neumann problems for Partial Differential Equations. The above method includes a least squares formulation and is fairly easy to implement using finite element approximations. We shall discuss first application to linear elliptic equations and then to the full potential equation modelling compressible inviscid flow, including cases where the flow is supersonic in the far field. Numerical results validating the above approach are given, and show that the method is robust, accurate and easy to implement.

1. Introduction and Synopsis

This article can be considered as a sequel of a lecture given at the *Fourth International Conference on Domain Decomposition Methods for Partial Differential Equations.* It was shown there that least squares and finite element methods can be combined to *domain imbedding* (i.e. *fictitious domain*) techniques to solve efficiently *Neumann problems* in domains of (almost) arbitrary shape. This method which has some commonality with the methods described in [1] is not without complication, particularly while computing accurately the various integrals associated to the present approach which is based on variational principles.

[1]University of Houston, Department of Mathematics, Houston, Texas 77204-3476.
[2]Dassault Aviation, Saint-Cloud, France.
[3]University of Houston, Department of Mathematics, Houston, Texas 77204-3476, Université P. et M. Curie, Paris and INRIA, France.
[4]Dassault Aviation, Saint-Cloud and Université P. et M. Curie, Paris, France.

Basic fictitious domain methods for elliptic problems are discussed in e.g. [2], [3], [4] (see also the references therein); application to transonic flow by related methods is discussed in [5].

In the present paper we shall discuss first (in Section 2) the application of a domain imbedding method to the solution of *Neumann problem, for linear elliptic equations*, and then generalize (in Section 3) the methodology to a class of much more complicated problems, namely the numerical solution of the *full potentiall equation* modelling the *potential transonic flow of compressible inviscid fluids*, including test cases for flow supersonic at infinity.

2. A least square domain imbedding method for linear Neumann problems.

2.1 Formulation. Generalities.

Motivated by the solution of Neumann problems occurring in applications such as *Fluid Dynamics* and *Petroleum Engineering* we consider the following problem

$$-\nabla\cdot\overline{\overline{A}}\nabla u + a_0 u = f \text{ in } \omega, \tag{2.1}$$

$$\overline{\overline{A}}\nabla u\cdot n = g \text{ on } \gamma. \tag{2.2}$$

In (2.1), (2.2), ω is a bounded domain of $\mathbb{R}^d (d\geq 1)$ and γ is its boundary; the functions f and g are given and defined over ω and γ, respectively; vectors ∇ and n are $\left\{\frac{\partial}{\partial x_i}\right\}_{i=1}^d$ and the unit outward normal vector at γ, respectively, and $a\cdot b=\sum_{i=1}^d a_i b_i$, $\forall a=\{a_i\}_{i=1}^d$, $b=\{b_i\}_{i=1}^d$; finally a_0 and $\overline{\overline{A}}$ satisfy the following conditions:

$$a_0\in L^\infty(\omega),\ a_0 \geq 0 \text{ a. e. on } \omega, \tag{2.2}$$

$$\overline{\overline{A}}\in\left(L^\infty(\omega)\right)^{d^2};\ \overline{\overline{A}}(x)\xi\cdot\xi \geq c|\xi|^2, \text{ a. e. on } \omega,\ \forall\xi\in\mathbb{R}^d, \tag{2.3}$$

with (in (2.3)) $c>0$ and $|\xi|^2=\sum_{i=1}^d \xi_i^2$, $\forall\xi=\{\xi_i\}_{i=1}^d$.

It follows from, e.g., [6, Appendix 1] that problem (2.1), (2.2) has a unique solution in $H^1(\omega)$ if $a_0 \neq 0$ and if f and g are sufficiently smooth (if $a_0 = 0$, problem (2.1), (2.2) has a unique solution defined within to an additive constant if and only if

$$\int_{\omega} f dx + \int_{\gamma} g d\gamma = 0, \tag{2.4}$$

with $dx = dx_1, \ldots, dx_d$). It follows from [6] that (2.1), (2.2) is equivalent to the following *variational problem*

$$\begin{cases} u \in H^1(\omega), \\ \int_{\omega} (a_0 uv + \bar{\bar{A}} \nabla u \cdot \nabla v) dx = \int_{\omega} fv dx + \int_{\gamma} gv d\gamma, \ \forall v \in H^1(\omega). \end{cases} \tag{2.5}$$

2.2 A fictitious domain approach to the solution of problem (2.1), (2.2).

Let us imbed domain ω in a "box" Ω, with boundary Γ, as shown in Figure 2.1 below.

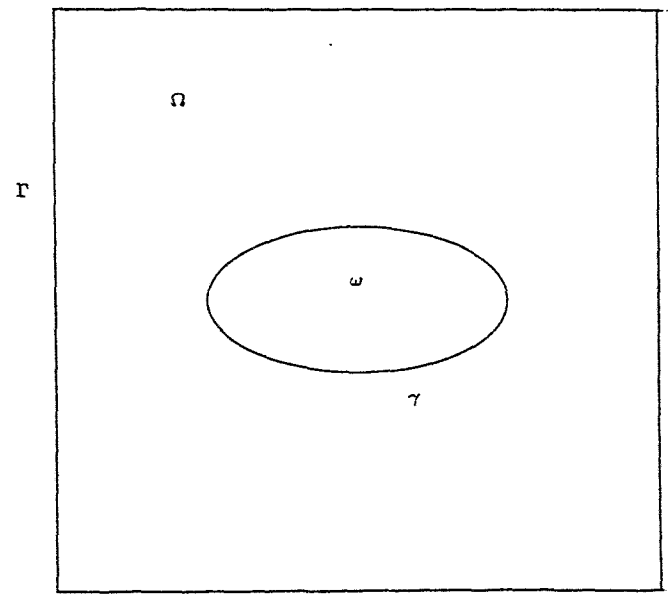

Figure 2.1 (imbedding of ω in Ω)

Next we introduce V such that

(2.6) V *is a closed subspace of* $H^1(\Omega)$,

(2.7) $V|_\omega = H^1(\omega)$.

Natural candidates for V are $H^1(\Omega)$, $H^1_0(\Omega)$ and the space $H^1_P(\Omega)$ defined by

(2.8) $H^1_P(\Omega) = \{v | v \in H^1(\Omega),\ v \text{ periodic at } \Gamma\}$.

Problem (2.1), (2.2), (2.5) is clearly equivalent to

(2.9) $$\int_\Omega (\alpha yz + \nabla y \cdot \nabla z)dx = \int_\omega (\bar{\bar{A}}\nabla u \cdot \nabla z + a_0 uz)dx - \int_\omega fzdx - \int_\gamma gzd\gamma,\ \forall z \in V,\ y \in V,$$

(2.10) $y = 0$,

in the sense that if a function $u \in H^1(\omega)$ verifies (2.9), (2.10) it is clearly the solution of (2.5), and conversely (in (2.9), α has to be *positive* if $V = H^1(\Omega)$ or $H^1_P(\Omega)$; it can be taken *equal to zero* if $V = H^1_0(\Omega)$).

Problem (2.9), (2.10) has the following block structure

(2.11) $$\begin{cases} Ay + Bv = b \\ \\ y = 0 \end{cases}$$

where, in (2.11), $A \in \mathcal{L}(V, V')$, $B \in \mathcal{L}(H^1(\omega), V')$, $b \in V'$. Since $V|_\omega = H^1(\omega)$, we can take $B \in \mathcal{L}(V, V')$ in (2.11); we use this alternative possibility in (2.12), below.

To solve problem (2.9), (2.10), we can use the following *least squares* formulation

(2.12) $$\operatorname*{Min}_{v \in V} J(v),$$

where, in (2.12), J(v) is defined as follows:

$$J(v) = \frac{1}{2}\int_{\Omega} (\alpha|y|^2 + |\nabla y|^2)dx, \tag{2.13}$$

with $y(=y(v))$ *the* solution of

$$\begin{cases} y \in V, \\ \int_{\Omega} (\alpha yz + \nabla y \cdot \nabla z)dx = \int_{\omega} (\bar{\bar{A}}\nabla v \cdot \nabla z + a_0 vz)dx - \int_{\omega} fzdx - \int_{\gamma} gzd\gamma, \ \forall z \in V. \end{cases} \tag{2.14}$$

Remark 2.1: Problem (2.12)−(2.14) has the structure of an *Optimal Control Problem* in the sense of J. L. Lions [7]; here v is the *control* variable and y is the *state* variable.

Remark 2.2: In the above formulation we have taken the control and state functions in the same space V. Actually, this is not necessary as long as *the control space restricted* to ω coincides with $H^1(\omega)$.

Remark 2.3: A main motivation of the fictitious domain approach is that it allows the use of fairly *structured meshes* in the box Ω, allowing therefore the use of fast solvers, like those based on *cyclic reduction* (see references 8 to 14 in the companion paper [1]). □

Concerning the well posedness properties of problem (2.12) we can prove easily the following

Theorem 2.1: *Problem* (2.1) *has a unique solution in the quotient space* $V/\mathcal{R}$, *where the equivalence relation* $\mathcal{R}$ *is defined by*

$$v\mathcal{R}w \Leftrightarrow v = w \text{ on } \omega. \tag{2.15}$$

This solution restricted to ω *coincides with the solution of* (2.1), (2.2), (2.5) *and the corresponding value of* y *is zero.*

In the following paragraphs we shall discuss the *conjugate gradient* solution of problem (2.12) – (2.14).

2.3 Conjugate Gradient Solution of the Least Squares Problem (2.12)–(2.14).

The *conjugate gradient* algorithm that we apply to the solution of (2.12)–(2.14) is the following (classical) one:

(2.16) $u^0 \in V$ *is given.*

Solve

$$(2.17)\qquad \begin{cases} g^0 \in V, \\ \displaystyle\int_\Omega (\alpha g^0 z + \nabla g^0 \cdot \nabla z)dx = \langle J'(u^0), z\rangle, \ \forall z \in V, \end{cases}$$

and set

(2.18) $w^0 = g^0$. □

Then for $n \geq 0$, u^n, g^n, w^n *being known, compute* u^{n+1}, g^{n+1}, w^{n+1} *as follows:*

Solve

$$(2.19)\qquad \begin{cases} \rho_n \in \mathbf{R}, \\ J(u^n - \rho_n w^n) \leq J(u^n - \rho w^n), \ \forall \rho \in \mathbf{R}, \end{cases}$$

and compute

(2.20) $u^{n+1} = u^n - \rho_n w^n$.

Solve

$$(2.21)\qquad \begin{cases} g^{n+1}\in V, \\ \int_\Omega (\alpha g^{n+1} z + \nabla g^{n+1}\cdot\nabla z)dx = \langle J'(u^{n+1}), z\rangle, \ \forall z\in V. \end{cases}$$

If $\|g^{n+1}\|_V/\|g^o\|_V\le\epsilon$ *take* $u=u^{n+1}$; *if not, compute*

$$(2.22)\qquad \gamma_n = \frac{\|g^{n+1}\|_V^2}{\|g^n\|_V^2},$$

and then

$$(2.23)\qquad u^{n+1} = g^{n+1} + \gamma_n w^n. \quad \square$$

Do $n=n+1$ *and go to* (2.19). $\square$

In (2.16)–(2.23), $\langle\cdot,\cdot\rangle$ denotes the *duality pairing* between V' and V and $\|v\|_V$ is defined by

$$(2.24)\qquad \|v\|_V^2=\int_\Omega (\alpha v^2+|\nabla v|^2)dx.$$

Concerning $J'(v)$, we can easily show that

$$(2.25)\qquad \langle J'(v), w\rangle = \int_\omega (\bar{\bar{A}}\nabla w\cdot\nabla y + a_o yw)dx, \ \forall w\in V,$$

where, in (2.25), y is the solution of (2.14).

Taking (2.25) into account, and also the fact that the mapping $v\longrightarrow J'(v)$ is *affine* from V into V' algorithm (2.16)–(2.23) can be written in the following (more practical) form:

$$(2.26)\qquad u^o\in V;$$

solve

$$(2.27)\qquad \begin{cases} y^o \in V, \\ \displaystyle\int_\Omega (\alpha y^o z + \nabla y^o \cdot \nabla z)dx = \int_\omega (\bar{\bar{A}} \nabla u^o \cdot \nabla z + a_o u^o z)dx - \int_\omega fz dx - \int_\gamma gz d\gamma, \ \forall z \in V, \end{cases}$$

and then

$$(2.28)\qquad \begin{cases} g^o \in V, \\ \displaystyle\int_\Omega (\alpha g^o z + \nabla g^o \cdot \nabla z)dx = \int_\omega (\bar{\bar{A}} \nabla z \cdot \nabla y^o + a_o y^o z)dx, \ \forall z \in V, \end{cases}$$

and set

$$(2.29)\qquad w^o = g^o. \quad \square$$

Then, for $n \geq 0$, *assuming that* u^n, y^n, g^n, w^n *are known we compute* u^{n+1}, y^{n+1}, g^{n+1}, w^{n+1} *as follows:*

Solve

$$(2.30)\qquad \begin{cases} \bar{y}^n \in V, \\ \displaystyle\int_\Omega (\alpha \bar{y}^n z + \nabla \bar{y}^n \cdot \nabla z)dx = \int_\omega (\bar{\bar{A}} \nabla w^n \cdot \nabla z + a_o w^n z)dx, \ \forall z \in V, \end{cases}$$

and then

$$(2.31)\qquad \begin{cases} \bar{g}^n \in V, \\ \displaystyle\int_\Omega (\alpha \bar{g}^n z + \nabla \bar{g}^n \cdot \nabla z)dx = \int_\omega (\bar{\bar{A}} \nabla z \cdot \nabla \bar{y}^n + a_o \bar{y}^n z)dx, \ \forall z \in V, \end{cases}$$

Compute now

$$\rho_n = \frac{\|g^n\|_V^2}{\int_\Omega (\alpha \bar{g}^n w^n + \nabla \bar{g}^n \cdot \nabla w^n) dx}, \tag{2.32}$$

and then

$$u^{n+1} = u^n - \rho_n w^n, \tag{2.33}$$

$$y^{n+1} = y^n - \rho_n \bar{y}^n, \tag{2.34}$$

$$g^{n+1} = g^n - \rho_n \bar{g}^n. \tag{2.35}$$

If $\|g^{n+1}\|_V / \|g^o\|_V \leq \epsilon$ *take* $u = u^{n+1}$; *if not compute*

$$\gamma_n = \frac{\|g^{n+1}\|_V^2}{\|g^n\|_V^2}, \tag{2.36}$$

and then

$$w^{n+1} = g^{n+1} + \gamma_n w^n. \quad \square \tag{2.37}$$

Do $n = n+1$ *and go to* (2.30).

Remark 2.4: Due to the least squares approach, another natural stopping criterion is defined by

$$\|y^{n+1}\|_V \Big/ \|y^o\|_V \leq \epsilon,$$

since $\|y^n\|_V$ is the square root of the *least square residual* that we are trying to force to vanish.

For more information about least square methods we recommend the review paper by A. Bjorck [8].

2.4 Finite Element Implementation of the Imbedding Method.

Let V_h be a finite dimensional subspace of V. We approximate the least squares problem (2.12)–(2.14) by

$$\text{(2.38)} \qquad \operatorname*{Min}_{v_h \in V_h} J_h(v_h),$$

where, in (2.38), $J_h(v_h)$ is defined as follows

$$\text{(2.39)} \qquad J_h(v_h) = \frac{1}{2}\int_\Omega (\alpha|y_h|^2 + |\nabla y_h|^2)dx,$$

with $y_h\big(=y_h(v_h)\big)$ *the* solution of

$$\text{(2.40)} \qquad \begin{cases} y_h \in V_h, \\ \displaystyle\int_\Omega (\alpha y_h z_h + \nabla y_h \cdot \nabla z_h)dx = \int_\omega (\bar{\bar{A}}\nabla v_h \cdot \nabla z_h + a_o v_h z_h)dx - \int_\omega f z_h - \int_\gamma g z_h d\gamma, \ \forall z_h \in V_h. \end{cases}$$

From a numerical point of view the main issue is the ability to compute easily and accurately the various integrals occurring in the right hand side of the variational equation in (2.40).

In the particular case of *finite element* approximations it seems essential that the *singular* points of γ coincide with vertices (or edges) or the finite element mesh.

The least squares problem (2.38)–(2.40) can be solved by a conjugate gradient algorithm which is a simple finite dimensional variant of algorithm (2.26)–(2.37).

2.5 Numerical Experiments.

We consider the particular case of problem (2.1), (2.2) defined by

$$\text{(2.41)} \qquad -\Delta u + u = f \text{ in } \omega,$$

$$\frac{\partial u}{\partial n} = g \text{ on } \gamma, \tag{2.42}$$

with $\omega=(.25, .75)^2$. The data f and g have been determined in such a way that *the* solution of (2.41), (2.42) is given by

$$u(x_1, x_2) = \sin 2\pi x_1 \sin 2\pi x_2. \tag{2.43}$$

Domain ω has been imbedded in $\Omega=(0,1)^2$ as shown in Figure 2.2, which also shows a particular finite element triangulation used for our calculations (on Figure 2.2 we have $h=1/4$). Problem (2.1), (2.2) has been solved using the methodology described in Sections 2.2 to 2.4.

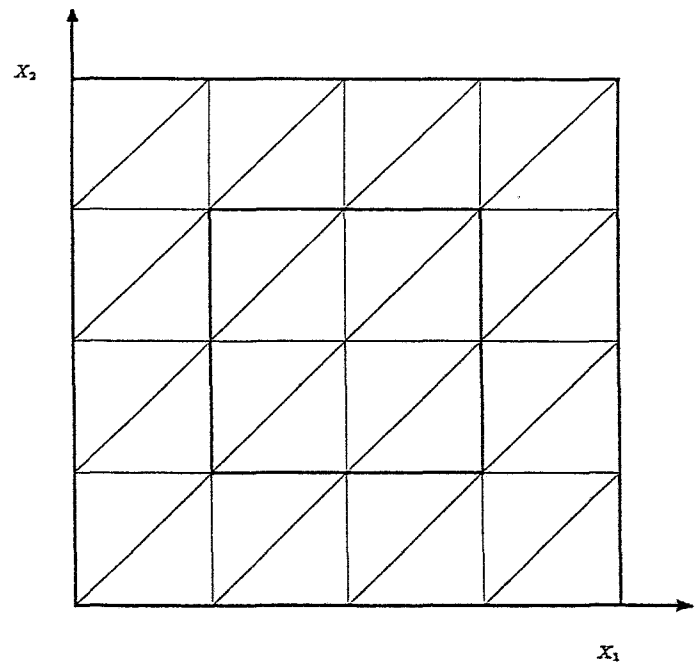

Figure 2.2

In the following Table 2.1 we give the number of iterations necessary for convergence with $\epsilon=10^{-7}$ and the error $\|u_h-u\|_\infty$ versus h.

h	Iteration number	$\|u_h - u\|_\infty$
$\frac{1}{8}$	5	1.80
$\frac{1}{16}$	9	.46
$\frac{1}{32}$	11	.12
$\frac{1}{64}$	12	$.30\times10^{-1}$

Table 2.1

From this table we observe that the approximation is $O(h^2)$ and that for h sufficiently small the number of iterations is independent of h (indeed the L^2—errors are much smaller).

In the following Section 3 we shall generalize the methodology discussed in this section to the numerical solution of a much more complicated nonlinear problem.

3. Fictitious Domain Methods for Transonic Potential Flow Calculations.

3.1 Generalities.

In this section, which is largely inspired by [9] we (briefly) consider the solution of a *Neumann problem* for an operator which is not only *nonlinear* but also of *mixed type*, namely *elliptic-hyperbolic*, if some data is sufficiently large; these problems occur in the simulation of *transonic potential flow* for *inviscid compressible fluids.* If one takes an historical perspective, it is known that rectangular grids were used for the simulation of flow around bodies, and interpolation procedures were needed to take into account the body surface. Body-fitted meshes combined to conservative difference schemes have been a substantial improvement leading to accurate solutions for the Euler and Navier-Stokes equations simulating a large variety of fluid flows. However, real life flows are mostly around complex geometrical configurations and the task of generating a body-fitted mesh, either structured or

unstructured, can be very time-consuming and computer-intensive. Moreover, in the case of unsteady flow involving moving structures, remeshing is needed and can lead to an important increase in computer time. Generalizing Section 2, and following [9], we describe a fictitious domain finite element/least squares method which uses a cartesian grid (at least locally around the body) to simulate transonic potential flow. Numerical experiments will include flow with a nonzero angle of attack, which, in addition, are supersonic at infinite. It has to be understood that these calculations are really preliminary and the results were obtained very shortly after the methodology presented in Section 2 was introduced.

3.2 Mathematical formulation.

We consider the potential flow of a compressible inviscid fluid around the airfoil A shown in Figure 3.1, below.

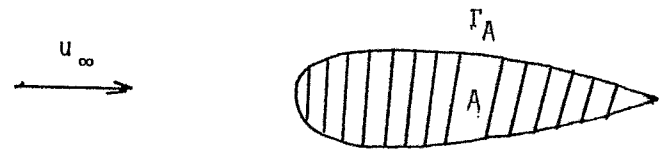

Figure 3.1

We denote by Γ_A the boundary of A and by ω the flow domain $\mathbf{R}^d/\bar{A}$. If the flow is potential it is modelled by

$$-\nabla\cdot(\rho\nabla\varphi) = 0 \text{ in } \omega, \tag{3.1}$$

$$\rho\frac{\partial\varphi}{\partial n} = 0 \text{ on } \Gamma_A, \tag{3.2}$$

(3.3) $\nabla\varphi = \mathbf{u}_\infty$ *at infinity,*

(3.4) $$\rho = \rho_0 \left(1 - \frac{\gamma-1}{\gamma+1} \frac{|\nabla\varphi|^2}{C_*^2}\right)^{1/(\gamma-1)}.$$

In (3.1)−(3.4), the potential φ and the velocity $\mathbf{u}$ are related by

(3.5) $$\mathbf{u} = \nabla\varphi,$$

ρ_0 is the fluid *density* at rest, γ is the *ratio of specific heats* (γ=1.4 for air) and C_* is the *critical velocity.* Relations (3.1)−(3.4) have to be completed by *entropy* and *Kutta-Joukowsky conditions* (see, e.g., [11]−[13] for details). Following the above references we bound the physical space by a large *artificial boundary* Γ_∞, on which we prescribe

(3.6) $$\rho \frac{\partial\varphi}{\partial n} = \rho_\infty \mathbf{u}_\infty \cdot \mathbf{n}_\infty$$

where $\rho_\infty = \rho_0\left(1 - \frac{\gamma-1}{\gamma+1} \frac{|\mathbf{u}_\infty|^2}{C_*^2}\right)^{1/(\gamma-1)}$ and where $\mathbf{n}_\infty$ is the unit outward normal vector at Γ_∞ (see Figure 3.2).

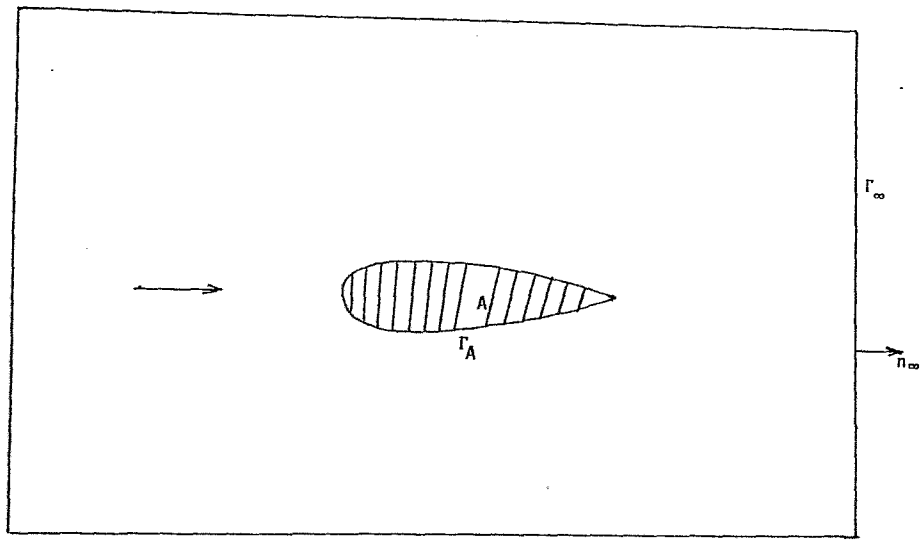

Figure 3.2

We still denote by ω the "truncated" flow domain.

3.3 A fictitious domain/least squares formulation.

Following Section 2 (and also [9] – [12]) we associate to problem (3.1)–(3.4) the following (*nonlinear*) least squares/domain imbedding problem

$$\text{(3.7)} \qquad \operatorname*{Min}_{v\in V} J(v),$$

where, in (3.7), with Ω=interior of closure of $A\cup\omega$,

$$\text{(3.8)} \qquad J(v) = \frac{1}{2}\int_{\Omega} (\alpha y^2 + |\nabla y|^2)dx,$$

$$\text{(3.9)} \qquad \int_{\Omega} (\alpha yz + \nabla y\cdot\nabla z)dx = \int_{\omega}\rho(v)\nabla v\cdot\nabla z dx - \int_{\Gamma_A\cup\Gamma_\infty} gzd\gamma,\ \forall z\in V,$$

with $g=0$ on Γ_A, $g=\rho_\infty u_\infty\cdot n_\infty$ on Γ_∞.

In practice we have to include in the above formulation *entropy* and *Kutta-Joukowsky conditions* to eliminate nonphysical solutions; the implementation of these two conditions is discussed in [10]–[12] together with their finite element implementation. Indeed space V in (3.7)–(3.9) is a subspace of $H^1(\Omega)$, well suited to piecewise linear finite element approximations. Another approach, which is advocated in [9], is to use a combination of Newton's method and GMES algorithm (see [13]) to solve the system

$$\text{(3.10)} \qquad \begin{cases} \displaystyle\int_{\omega}\rho(u_h)\nabla u_h\cdot\nabla z_h dx - \int_{\Gamma_\infty} gzd\gamma,\ \forall z\in V_h, \\ u_h\in V_h, \end{cases}$$

where, in (3.10), V_h is a well-chosen finite element space. This formulation has the advantage of being applicable to flows which are supersonic at infinity through nonsymmetric indefinite preconditioning operators reflecting the dominating *hyperbolic character* of the operator $\nabla\cdot\rho(\varphi)\nabla\varphi$ (see [9] for further comments).

3.4 Numerical results.

All the test problems considered here correspond to transonic potential flow around a NACA 0012 airfoil. Three test cases have been considered corresponding to M_∞=.8, .95, 1.2 and α=1°, 0, 2°, respectively (α: angle of attack). These test cases are interesting since they correspond to lifting situations and large supersonic regions. The fictitious domain results have been compared to finite element ones based on body-fitted triangulations.

First Test Problem: We have M_∞=.8 and α=1°. Part of the finite element mesh used for the fictitious domain approach (resp. the comparison calculation) is shown on Figure 3.3 (resp. Figure 3.4). Piecewise linear approximations have been used for both calculations. Figures 3.5 and 3.6 show the Mach contours for the fictitious domain and comparison calculations, respectively. Similarly with Figures 3.7 and 3.8 for the pressure contours. A comparison between Mach and pressure distributions on the airfoil is shown on Figures 3.9 and 3.10, respectively. The fictitious domain results have been obtained after twenty iterations corresponding to computational time of 3.5 minutes on an IBM 3090 computer. Present and Reference solutions agree quite well.

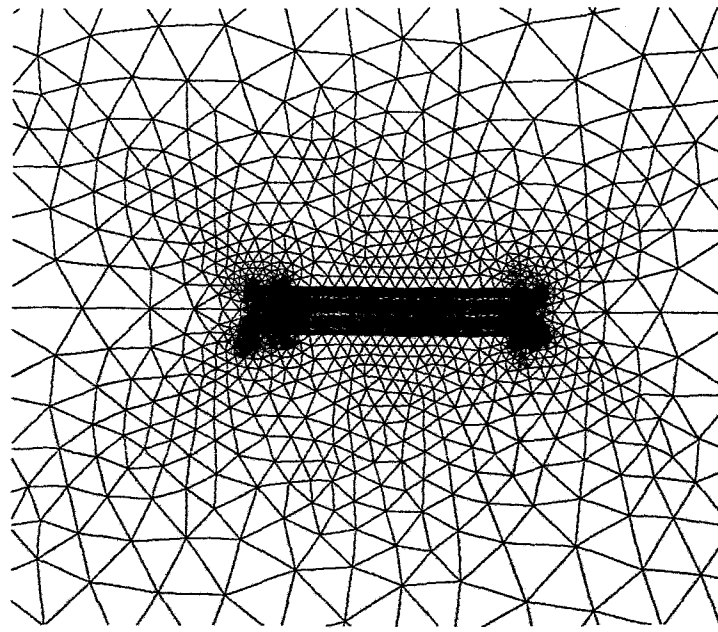

Figure 3.3

Fictitious Domain Method Triangulation (1937 vertices, 3836 triangles)

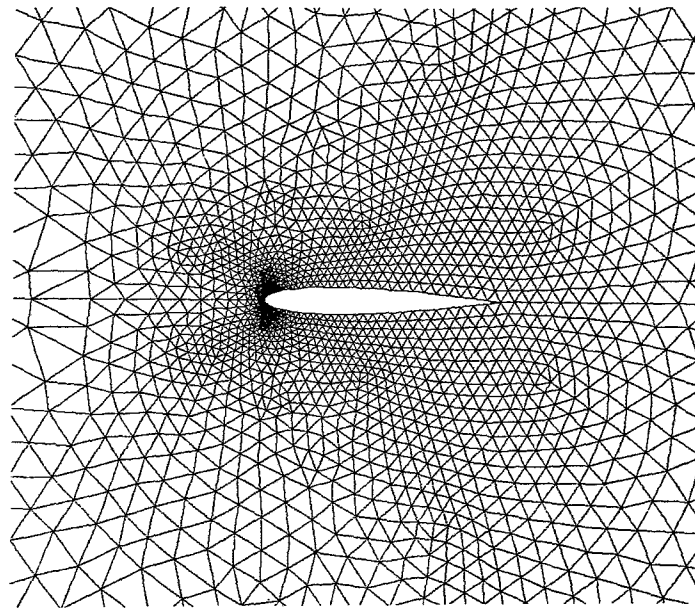

Figure 3.4

Part of the Comparison Calculation Triangulation (3114 vertices, 6056 triangles)

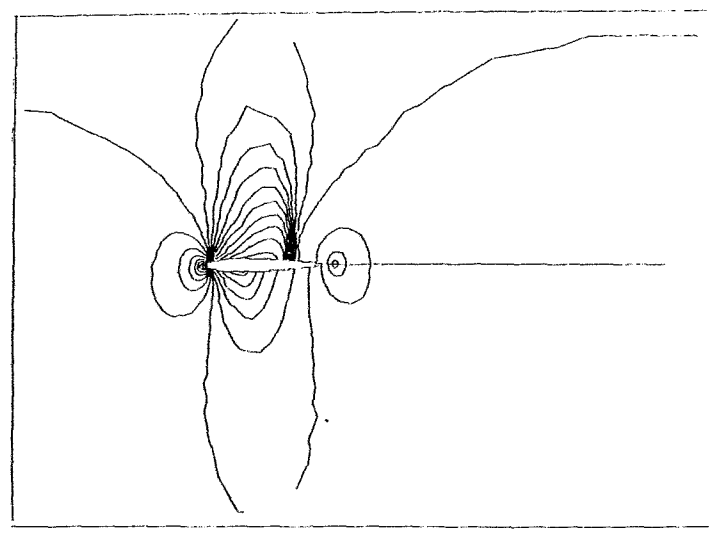

Figure 3.5

Fictitious Domain Calculation: Mach Distribution ($M_\infty = .8$, $\alpha = 1^\circ$)

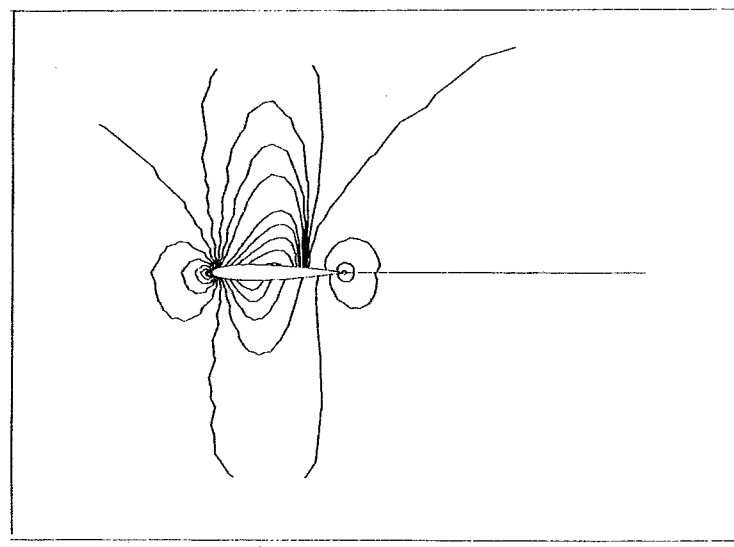

Figure 3.6

Comparison Calculation: Mach Distribution ($M_\infty = .8$, $\alpha = 1^\circ$)

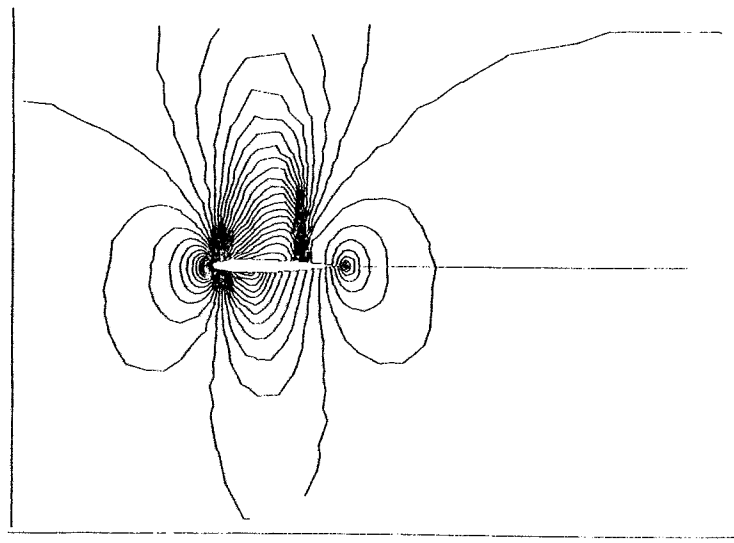

Figure 3.7

Fictitious Domain Calculation: C_p Distribution ($M_\infty = .8$, $\alpha = 1^\circ$)

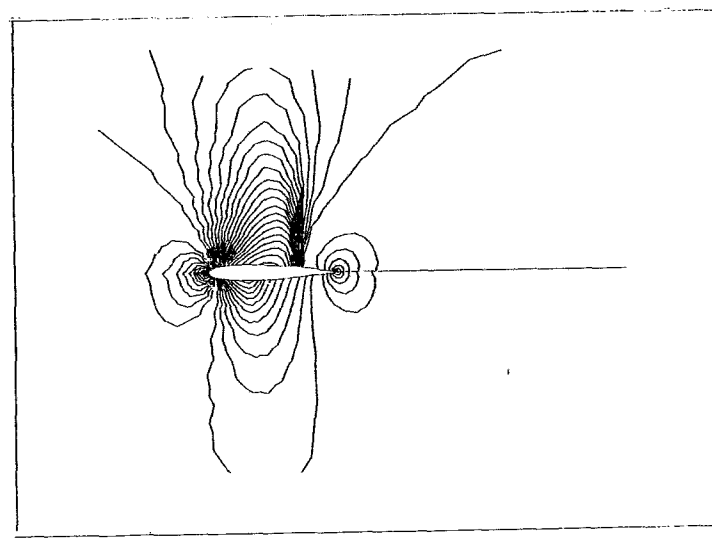

Figure 3.8

Comparison Calculation: C_p Distribution ($M_\infty = .8$, $\alpha = 1^\circ$)

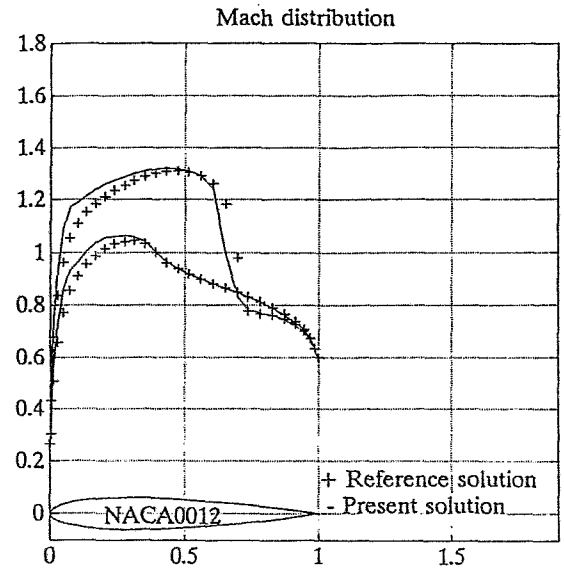

Figure 3.9

Mach Distribution Comparison ($M_\infty = .8$, $\alpha = 1^\circ$)

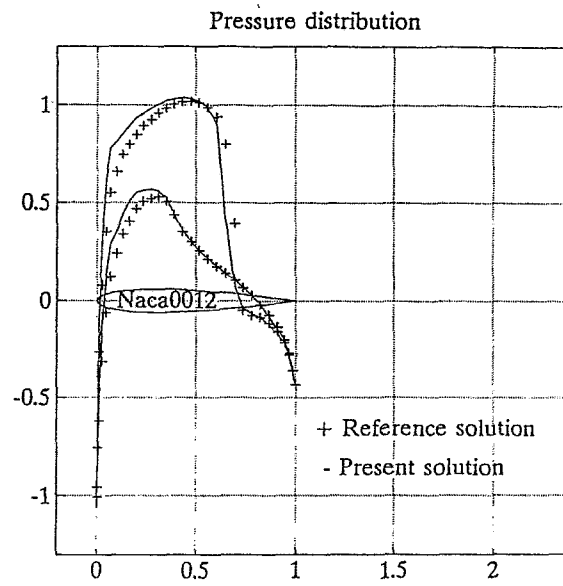

Figure 3.10

Pressure Distribution Comparison (M_∞=.8, α=1°)

Second Test Problem: We have M_∞=.95, α=0°. The finite element grids used in this test case are those of Figures 3.3, 3.4. On Figures 3.11 to 3.13 we have shown and compared the results obtained by the fictitious domain approach and by the body-fitted finite element approximation.

For this fully transonic case the agreement between both calculations is still quite good.

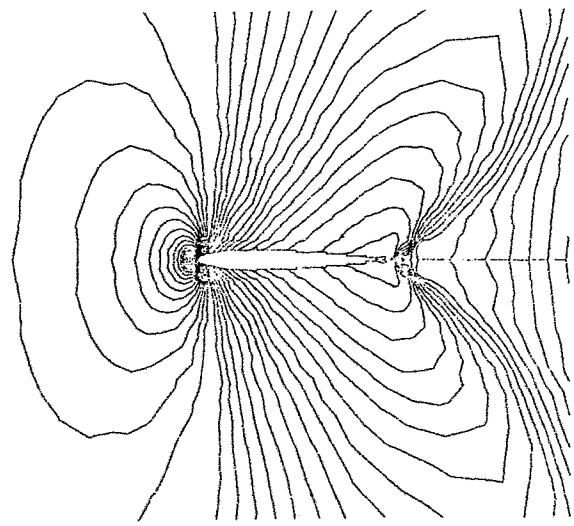

Figure 3.11

Fictitious Domain Calculation: Pressure Distribution (M_∞=.95, α=0°)

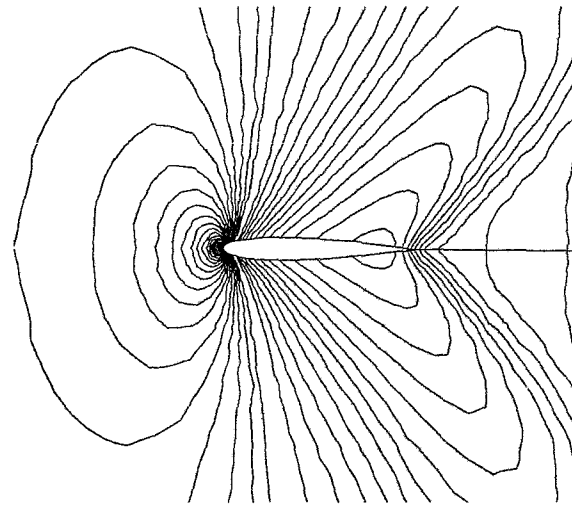

Figure 3.12

Comparison Calculation: Pressure Distribution ($M_\infty = .95$, $\alpha = 0°$)

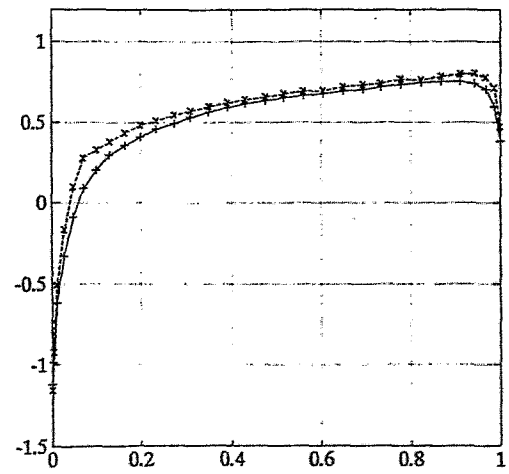

Figure 3.13

Pressure Distribution Comparison ($M_\infty = .95$, $\alpha = 0°$)
(×: fictitious domain calculation; +: comparison calculation)

Third Test Problem: We have $M_\infty=1.2$, $\alpha=2^\circ$. The finite element grids used in this test case are still those of Figures 3.3, 3.4. This case is more difficult than the above two since it concerns a transonic flow supersonic at infinity. On Figures 3.14 to 3.16 we have shown the results obtained by the fictitious domain approach and by the body-fitted finite element approximation.

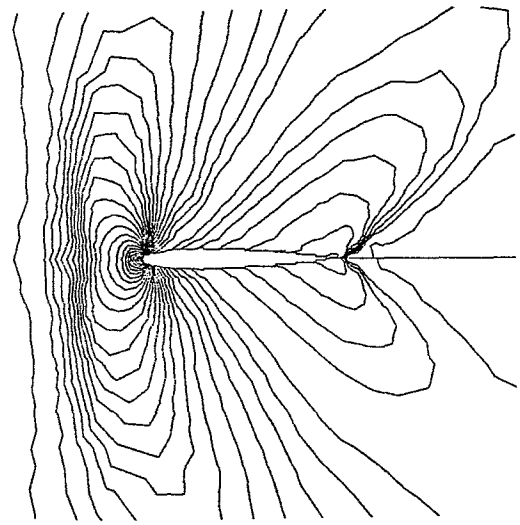

Figure 3.14

Fictitious Domain Calculation: Pressure Distribution ($M_\infty=1.2$, $\alpha=2^\circ$)

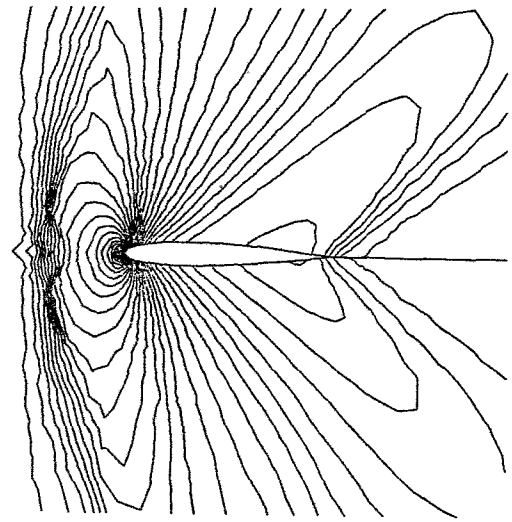

Figure 3.15

Comparison Calculation: Pressure Distribution ($M_\alpha=1.2$, $\alpha=2^\circ$)

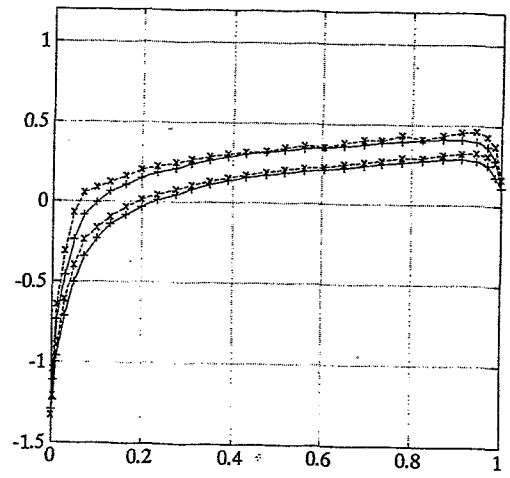

Figure 3.16

Pressure Distribution Comparison (M_∞=1.2, α=2°)
(×: fictitious domain calculation; +: comparison calculation)

From the above three test cases we can say that we have a fairly good agreement for the nomal shocks, the two oblique shocks and the bow shock. However, further refinement seems needed at the trailing edge, particularly for cases 2 and 3 where shocks are located there.

4. Conclusion

We have introduced here a fictitious domain methodology for partial differential equation problems with Neumann boundary conditions. From the results obtained with the compressible flow problem discussed in Section 3, we can say that the method looks promissing. It is much easier to code than a finite element method using a body fitted mesh. Indeed the method described in this article is still in its preliminary phases, and we can expect various improvements.

Acknowledgment

We would like to acknowledge the helpful comments and suggestions of the following individuals: C. Atamian, L. C. Cowsar, C. De la Foye, G. H. Golub, P. Joly, Y. Kuznetsov, A. Latto, W. Lawton, P. Le Tallec, J. L. Lions, P. L. Lions, G. Meurant, J. Pasciak, M. Ravachol, H. Resnikoff, H. Steve, J. Weiss, R. O. Wells, M. F. Wheeler, O. B. Widlund.

The support of the following corporations or institutions is also acknowledged: AWARE, Dassault Aviation, INRIA, University of Houston, Université Pierre et Marie Curie. We also benefited from the support of DARPA (Contracts AFOSR F49620-89-C-0125 and AFOSR-90-0334), DRET (Grant 89424) and NSF (Grants INT 8612680 and DMS 8822522). Finally, we would like to thank J. A. Wilson for the processing of this article.

References

[1] Q. V. DINH, R. GLOWINSKI, J. HE, V. KWOCK, T. W. PAN and J. PERIAUX, Lagrange Multiplier Approach to Fictitious Domain Methods: Application to Fluid Dynamics and Electro-Magnetics (these Proceedings).

[2] W. PROSKUROWSKY and O. B. WIDLUND, On the numerical solution of Helmholtz equation by the capacitance matrix method, *Math. Comp.*, 30, (1979), pp. 433-468.

[3] D. P. O'LEARY and O. B. WIDLUND, Capacitance matrix methods for the Helmholtz equation on general three-dimensional regions, *Math. Comp.*, 30, (1979), pp. 849-879.

[4] G. I. MARCHUK and Y. A. KUZNETSOV, A. M. MATSOKIN, Fictitious domain and domain decomposition methods, *Sov. J. Num. Anal. Math. Modelling*, 1, (1986), pp. 3-35.

[5] D. P. YOUNG, R. G. MELVIN, M. B. BIETERMAN, F. T. JOHNSON, S. S. SAMANTH, and J. E. BUSSOLETTI, A locally refined finite rectangular grid finite element method. Application to Computational Physics, *J. Comp. Physics*, 92, (1991), pp. 1-66.

[6] R. GLOWINSKI, *Numerical Methods for Nonlinear Variational Problems*, Springer-Verlag, New York, 1984.

[7] J. L. LIONS, *Contrôle Optimal des systèmes gouvernés par des équations aux dérivées partielles*, Dunod, Paris, 1969.

[8] A. BJORCK, Least Squares Methods, in *Handbook of Numerical Analysis, Vol.* I, P. G. Ciarlet, J. L. LIONS, eds., North-Holland, Amsterdam, 1990, pp. 465-652.

[9] Q. V. DINH and J. W. HE, A Cartesian grid finite element method for potential flows, in *High Performance Computing* II, M. Durand, F. El Dabaghi eds., North-Holland, Amsterdam, 1991, pp. 295-306.

[10] M. O. BRISTEAU, R. GLOWINSKI, J. PERIAUX, P. PERRIER and G. POIRIER, Transonic flow simulations by finite element and least square methods, in *Finite Elements in Fluids*, Vol. 4, R. H. Gallagher, D. H. Norrie, J. T. Oden, O. C. Zienkiewicz, Wiley, Chichester, 1982, pp. 453-482.

[11] M. O. BRISTEAU, R. GLOWINSKI, J. PERIAUX, O. PIRONNEAU and G. POIRIER, On the numerical solution of nonlinear problems in fluid dynamics by least squares and finite element methods (II). Application to transonic flow simulations, *Computer Methods in Applied Mechanics and Engineering*, 51, (1985), pp. 363-394.

[12] M. O. BRISTEAU, R. GLOWINSKI, J. PERIAUX, P. PERRIER, O. PIRONNEAU, and G. POIRIER, Transonic Flow and Shock Waves: Least-squares and Conjugate Gradient Methods, in Section 4.3 of Part 3 of *Finite Element Handbook*, H. Kardestuncer, D. H. Norrie eds., McGraw-Hill, New York, 1987, pp. 3.229 - 3.243.

[13] Y. SAAD and M. H. SHULTZ, GMRES: A generalized minimal residual algorithm for solving non symmetric linear systems, *SIAM J. Sci. Stat. Comp.*, 7, (1986), pp. 856-